CHARACTERISING ROOM TEMPERATURE THz METAL SHIELDING USING THE ENGINEERING APPROACH

S. Lucyszyn and Y. Zhou

Optical and Semiconductor Devices Group
Department of EEE
Imperial College London
London, SW7 2AZ, United Kingdom

Abstract—This paper applies the recently introduced electrical engineering approach to investigate room temperature THz metal shielding, using the accurate classical relaxation-effect frequency dispersion model. It is shown that, with the simplest case of a uniform plane wave at normal incidence to an infinite single planar shield in air, all figure of merit parameters for the shield can be accurately characterized. The errors introduced by adopting the traditional and much simpler classical skin-effect model are also quantified. In addition, errors resulting from adopting well-established approximations have also been investigated and quantified. It is shown that the engineering approach allows analytical expressions to be greatly simplified and predictive equivalent transmission line models to be synthesized, to give a much deeper insight into the behaviour of room temperature THz metal shielding. For example, it is shown that figures of merit and associated errors (resulting from the use of different classical frequency dispersion models) become essentially thickness invariant when the physical thickness of the shield is greater than 3 normal skin depths.

1. INTRODUCTION

Radio frequency (RF) metal shielding is found in many applications; ranging from the construction of high isolation subsystem partitioning walls, efficient quasi-optical components (e.g., planar mirrors and parabolic reflectors for open resonators and antennas), creating guided-wave structures that have (near-) zero field leakage (e.g., metal-pipe rectangular waveguides and associated closed cavity resonators) and

---

Corresponding author: S. Lucyszyn (s.lucyszyn@imperial.ac.uk).

embedding ground planes within compact 3D multi-layer architectures. Ideally, metal shields should be made as thin as possible, while meeting the minimum values for figures of merit within the intended bandwidth of operation, in order to reduce weight and cost. For reasons of structural integrity, thin metal shielding can be deposited onto either a solid plastic/ceramic or even honeycomb supporting wall. Moreover, thin metal shielding embedded between dielectric layers (e.g., to create conformal ground planes or partition walls) can avoid issues of poor topography when integrating signal lines within 3D multi-layered architectures.

Shielding effectiveness, return loss and absorptance (or absorptivity) are important figures of merit that are quoted to quantify the ability to shield electromagnetic radiation. This paper will investigate these parameters for operation at terahertz frequencies. To describe the intrinsic frequency dispersion in metals for THz shielding applications, the accurate classical relaxation-effect model will be used as reference [1–6]. Differences between the results calculated for the classical skin-effect and relaxation-effect models will be quantified for a single planar shield, as previously undertaken with metal-pipe rectangular waveguide structures at terahertz frequencies [4, 6]. It will be assumed throughout that the intrinsic conductivity will be for a normal metal at room temperature and represented by its bulk values.

It has been recently shown that an electrical engineering approach, which can include network analysis and the synthesis of predictive equivalent transmission line models, can accurately solve specific electromagnetic problems [5, 6]. This approach will be used as a basic tool for the investigation of room temperature THz metal shielding.

2. S-PARAMETER ANALYSIS FOR SINGLE PLANAR SHIELD

For simplicity, an infinite single planar shield in air will be considered, with uniform plane wave at normal incidence, as illustrated in Fig. 1.

Within the metal, the propagation constant $\gamma \equiv \alpha + j\beta$, α is the attenuation constant and β is the phase constant. With reference to Fig. 1, at the respective dielectric $\rightarrow$ metal and metal $\rightarrow$ dielectric boundaries, the voltage reflection coefficients are:

$$\rho_1 = \frac{Z_S - Z_T}{Z_S + Z_T} \quad \text{and} \quad \rho_2 = \frac{Z_T - Z_S}{Z_S + Z_T} \equiv -\rho_1 \tag{1}$$

where $Z_S \equiv R_S + jX_S \rightarrow \eta_I = \sqrt{\frac{j\omega\mu}{\sigma + j\omega\varepsilon}}$ is the surface impedance of the metal, R_S is the surface resistance, X_S is the surface reactance and the termination impedance of this equivalent 2-port network
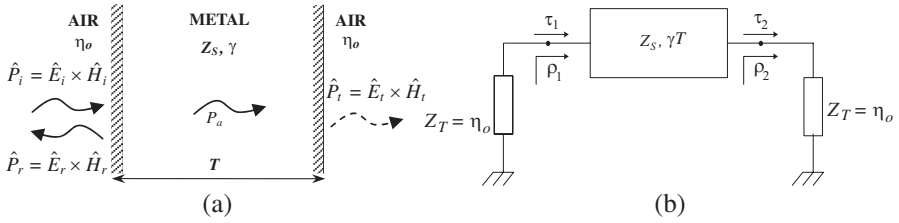
Figure 1. Uniform plane wave at normal incidence to an infinite single planar shield in air: (a) physical representation; and (b) equivalent 2-port network model.

$Z_T \rightarrow \eta_o = \sqrt{\frac{\mu_o}{\varepsilon_o}} \gg \eta_I$ is the intrinsic impedance of the surrounding air dielectric. The other variables have their usual meaning [1–6]. The corresponding voltage transmission coefficients are given by:

$$\tau_1 \equiv 1 + \rho_1 = \frac{2Z_S}{Z_S + Z_T} \quad \text{and} \quad \tau_2 \equiv 1 + \rho_2 = \frac{2Z_T}{Z_S + Z_T} \qquad (2)$$

The overall forward voltage-wave transmission coefficient S_{21} for this simple shielding scenario can be represented by the following transient response solution.

$$S_{21} = \tau_1 \cdot \left[e^{-\gamma T} \cdot \sum_{i=0}^{\infty} \left(e^{-\gamma T} \rho_2 \right)^{2i} \right] \cdot \tau_2 \quad \text{where} \quad i \in [0, 1, 2 \ldots \infty] \quad (3)$$

From (3), the steady-state solution is easily shown to be given by the following:

$$S_{21} = \tau_1 \cdot \left[\frac{e^{-\gamma T}}{1 - \left(e^{-\gamma T} \rho_1 \right)^2} \right] \cdot \tau_2 \quad \text{since} \quad \left| e^{-\gamma T} \rho_1 \right| < 1 \qquad (4)$$

Similarly, the overall input voltage-wave reflection coefficient S_{11} for this simple shielding scenario can be represented by the following transient response solution.

$$S_{11} = \rho_1 + \tau_1 \cdot \left[e^{-2\gamma T} \rho_2 \cdot \sum_{i=0}^{\infty} \left(e^{-\gamma T} \rho_2 \right)^{2i} \right] \cdot \tau_2 \text{ where } i \in [0, 1, 2 \ldots \infty] \quad (5)$$

From (5), the steady-state solution is easily shown to be given by the following:

$$S_{11} = \rho_1 \cdot \left[\frac{1 - e^{-2\gamma T}}{1 - \left(e^{-\gamma T} \rho_1 \right)^2} \right] \quad \text{since} \quad \left| e^{-\gamma T} \rho_1 \right| < 1 \qquad (6)$$

From the engineering approach, with a normal metal at room temperature, the effective component Q-factor $Q_c = \frac{X_S}{R_S} = \frac{\alpha}{\beta} \geq 1$ [5, 6]. As an extension to this approach, one can introduce the boundary resistance coefficient $k = \frac{\eta_o}{R_S} \gg Q_c \geq 1$. As a result, (1) and (2) can be represented as:

$$\rho_1 = \frac{(1-k) + jQ_c}{(1+k) + jQ_c} \approx 1; \quad \tau_1 = \frac{2(1+jQ_c)}{(1+k) + jQ_c} \cong \frac{2(1+jQ_c)}{k+jQ_c} \approx \frac{2(1+jQ_c)}{k};$$

$$\tau_2 = \frac{2k}{(1+k) + jQ_c} \cong \frac{2k}{k+jQ_c} \approx 2 \qquad (7)$$

It is useful to represent the physical thickness T of the metal shield in terms of the number a of normal skin depths $\delta_S = 1/\alpha$ (i.e., $T \to a\,\delta_S$). Thus, it can be easily shown that the exponential decay for the intensity of the electromagnetic fields within the metal can be represented by the following exponent [5]:

$$-\gamma T \to -\gamma \cdot a\,\delta_S = -a \cdot \left(1 + \frac{j}{Q_c}\right) \qquad (8)$$

Using the classical relaxation-effect model to describe frequency dispersion within a normal metal at room temperature [1–6], where associated variables for this model are indicated by the suffix "R", $T = a_R\,\delta_{SR}$. It is generally accepted that a metal wall of thickness equal to 5 normal skin depths is sufficient to provide acceptable power isolation for most applications. Therefore, the propagation constant per 5 skin depths becomes:

$$\gamma_R \cdot 5\delta_{SR} = 5\frac{\gamma_R}{\Im\{\gamma_R\}Q_{cR}} = 5\left(1 + \frac{j}{Q_{cR}}\right)\left[(5\delta_{SR})^{-1}\right] \qquad (9)$$

As an example, if an arbitrary frequency of $\omega\tau = 1$ is chosen, for simplicity, $Q_{cR}(\omega\tau = 1) = (1 + \sqrt{2})$ [5] and then (9) becomes:

$$\gamma_R(\omega\tau = 1) \cdot 5\delta_{SR}(\omega\tau = 1) = 5\left(1 + \frac{j}{1 + \sqrt{2}}\right)\left[(5\delta_{SR})^{-1}\right] \qquad (10)$$

Now, using the engineering approach, it can be shown respectively that (4) and (6) become:

$$
\begin{aligned}
S_{21R} &= \frac{4k_R \cdot (1+jQ_{cR}) \cdot e^{-a_R\left(1 + \frac{j}{Q_{cR}}\right)}}{[(1+k_R) + jQ_{cR}]^2 - [(1-k_R) + jQ_{cR}]^2 \cdot e^{-2a_R\left(1 + \frac{j}{Q_{cR}}\right)}} \\
&\approx \frac{2(1+jQ_{cR})}{k_R \cdot \sinh\left[a_R\left(1 + \frac{j}{Q_{cR}}\right)\right]}
\end{aligned}
\qquad (11)
$$

$$S_{11R} = \rho_{1R} \cdot \left[\frac{1 - e^{-2a_R\left(1 + \frac{j}{Q_{cR}}\right)}}{1 - \left(e^{-a_R\left(1 + \frac{j}{Q_{cR}}\right)}\rho_{1R}\right)^2} \right]$$

$$= \frac{\sinh\left[a_R\left(1 + \frac{j}{Q_{cR}}\right)\right]}{\sinh\left[a_R\left(1 + \frac{j}{Q_{cR}}\right) - \ln\left(\frac{(1-k_R)+jQ_{cR}}{(1+k_R)+jQ_{cR}}\right)\right]} \tag{12}$$

The approximation in (11) results in a worst-case error of less than 0.4% up to $a_R = 10$ and frequency less than 12 THz. Note that, since the voltage-wave reflection coefficient has a magnitude close to unity, it is not appropriate to simplify the expressions in (12). For the classical skin-effect model [1–6], where associated variables for this model are indicated by the suffix "o":

$$a_o = \frac{T}{\delta_{So}} = a_R \left(\frac{\delta_{SR}}{\delta_{So}}\right) \tag{13}$$

and it can be shown that (11) and (12) become:

$$S_{21o} = \frac{4\sqrt{2j}\,k_o \cdot e^{-a_o\sqrt{2j}}}{\left(\sqrt{2j} + k_o\right)^2 - \left(\sqrt{2j} - k_o\right)^2 \cdot e^{-2a_o\sqrt{2j}}} \approx \frac{2\sqrt{2j}}{k_o \cdot \sinh\left(a_o\sqrt{2j}\right)} \tag{14}$$

$$S_{11o} = \rho_{1o} \cdot \left[\frac{1 - e^{-2a_o\sqrt{2j}}}{1 - \left(e^{-a_o\sqrt{2j}}\rho_{1o}\right)^2}\right] = \frac{\sinh\left(a_o\sqrt{2j}\right)}{\sinh\left[a_o\sqrt{2j} - \ln\left(\frac{\sqrt{2j}-k_o}{\sqrt{2j}+k_o}\right)\right]} \tag{15}$$

The approximation in (14) results in a worst-case error of less than 0.6% up to $a_R = 10$ and frequency less than 12 THz.

2.1. Transmittance

The transmission power isolation that results from a shield can be defined by its shielding effectiveness (SE). With reference to Fig. 1(a), shielding effectiveness can be given separately for the electric (E) and magnetic (H) fields, SE_E and SE_H, respectively, [7]:

$$SE_E = 20\log_{10}\left|\frac{\overset{\wedge}{E_i}}{\overset{\wedge}{E_t}}\right| \text{ [dB]} \quad \text{and} \quad SE_H = 20\log_{10}\left|\frac{\overset{\wedge}{H_i}}{\overset{\wedge}{H_t}}\right| \text{ [dB]} \tag{16}$$

where the subscripts "i" and "t" denote the field strengths incident to and emanating from the other side of the shield, respectively. For a uniform plane wave at normal incidence to an infinite single planar shield, the shielding effectiveness for the electric and magnetic

fields coincide to give *SE*. With reference to Fig. 1(a), screening effectiveness (i.e., transmittance) is the fraction of incident power P_i to be transmitted past the shield P_t and is represented in decibels as:

$$SE_{\mathrm{dB}} = -10 \log_{10} \left(\frac{P_t}{P_i} \right) \ [\mathrm{dB}]$$

$$SE = \left\{ \begin{array}{ll} |S_{21R}|^2 & \textit{for all } a_R \\ \sim 0 & \textit{for } a_R > 3 \end{array} \right. \tag{17}$$

Shielding effectiveness is defined by the IEEE as "*the ratio of the signal received (from a transmitter) without the shield, to the signal received inside the shield; the insertion loss when the shield is placed between the transmitting antenna and the receiving antenna (IEEE Std 100–1996)*" [9]. Shielding effectiveness in decibels, SE_{dB}, can be determined using (4) and can be broken down into three separate terms; each representing the following phenomena of cross-boundary reflections R_{dB}, absorption A_{dB} and multiple reflections, M_{dB}:

$$SE_{\mathrm{dB}} = -20 \log_{10} \left| S_{21R} \cdot e^{+j\beta_o T} \right| = -20 \log_{10} |S_{21R}| \equiv R_{\mathrm{dB}} + A_{\mathrm{dB}} + M_{\mathrm{dB}} \tag{18}$$

where $\beta_o = \omega \sqrt{\mu_o \varepsilon_o}$ is the phase constant in free-space (the dielectric is assumed here to be air). R_{dB} is the combined transmission loss caused by the impedance mismatch reflections at the dielectric $\rightarrow$ metal and metal $\rightarrow$ dielectric boundaries:

$$R_{\mathrm{dB}} = -20 \log_{10} |\tau_{1R} \cdot \tau_{2R}| = 20 \log_{10} \left| \frac{(Z_{SR} + \eta_o)^2}{4 Z_{SR} \eta_o} \right|$$

$$\sim 20 \log_{10} \left| \frac{\eta_o}{4 Z_{SR}} \right| \rightarrow 20 \log_{10} \left| \frac{k_R}{4 (1 + j Q_{cR})} \right| \tag{19}$$

The well-known approximation in (19) is convenient when using the classical skin-effect model, because this calculation does not involve any complex numbers. However, it results in a worst-case error that increases with frequency, to a value of 6.8% at 12 THz for gold at room temperature. A_{dB} is the absorption (or penetration) loss of the electromagnetic energy as it propagates through the shield in the shortest path:

$$A_{\mathrm{dB}} = -20 \log_{10} \left| e^{-\gamma_R T} \right| = 20 \log_{10} \left(e^{T/\delta_{SR}} \right) \rightarrow 20 \log_{10} (e^{a_R}) \cong 8.686 a_R \tag{20}$$

The approximation in (20) gives a negligible worst-case error up to $a_R = 10$ and frequency less than 12 THz for gold at room temperature. M_{dB} is a correction factor that takes into account the

multiple (theoretically infinite) reflections between metal $\rightarrow$ dielectric boundaries:

$$M_{\mathrm{dB}} = = 20 \log_{10} \left| 1 - \left(e^{-\gamma_R T} \rho_{1R} \right)^2 \right| \sim 20 \log_{10} \left| 1 - e^{-2\gamma_R T} \right|$$
$$\rightarrow 20 \log_{10} \left| 1 - e^{-2a_R \cdot \left(1 + \frac{j}{Q_{cR}} \right)} \right| \tag{21}$$

The approximation in (21) has been cited by Paul [7]. It is worth noting that [8] takes even more extreme approximations, by ignoring the imaginary part of the exponent within the approximation in (21) for a thickness much less than the wavelength; while ignoring this correction factor altogether when thickness is much greater than the normal skin depth. These extreme approximations will not be considered further.

The correction factor for multiple reflections has been calculated for gold at room temperature using the classical relaxation-effect model. The results are represented by the contour plot shown in Fig. 2(a). The frequency range of interest is from dc to 12 THz; while that for physical thickness ranges from the mean-free path length l_m (i.e., $l_m = 37.9$ nm for gold at room temperature) to 10 normal skin depths. This lower limit of thickness tries to avoid any anomalous region of operation (as a point of reference, $\delta_{SR}(\omega\tau \cong 0.513) = l_m$ and so a_R increases from a value less than unity below $\omega\tau \cong 0.513$ but is always greater than unity above $\omega\tau \cong 0.513$).

It can be deduced from Fig. 2(a) that M_{dB} will have an adverse effect on screening effectiveness when the physical thickness approaches
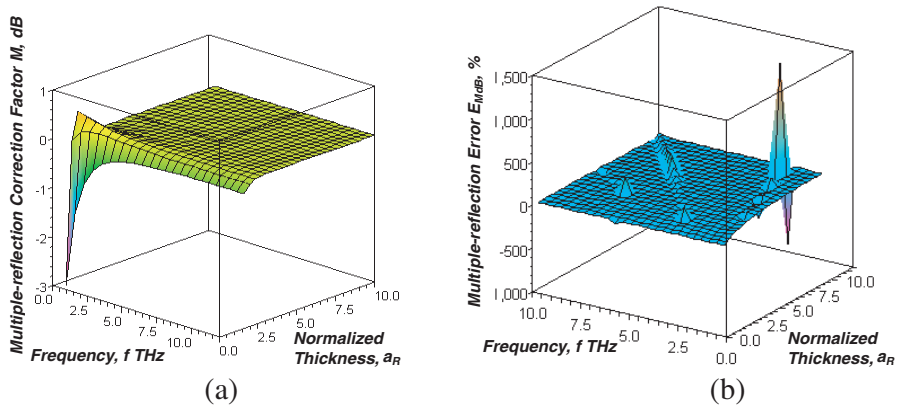
Figure 2. Correction factor for multiple reflections calculations: (a) using classical relaxation-effect model; (b) resulting error when using the approximation in (21).

the mean-free path length, i.e., $T \to l_m$. With large values of physical thickness there are fluctuations with $M_{\mathrm{dB}} \sim 0$. As a result, it will be seen that evaluating the worst-case error for the approximation in (21) is more problematic, using the following normal error equation, because of the singularities that are created (see Fig. 2(b)):

$$E_{M\mathrm{dB}} = \frac{M_{\mathrm{dB\_approximation}} - M_{\mathrm{dB\_exact}}}{M_{\mathrm{dB\_exact}}} \cdot 100\% \tag{22}$$

Using the exact expressions from (18) to (21) with (11), the overall shielding effectiveness has been calculated for gold at room temperature using the classical relaxation-effect model. The results are represented by the contour plot shown in Fig. 3(a). It can be seen that screening effectiveness SE_{dB} always decreases with increasing frequency, as more electromagnetic energy leaks through the shield. Moreover, as expected, it increases with physical thickness.

Note that if the results from the exact expressions are compared with the associated approximations, given in (19) to (21), then it is found that the worst-case error is less than 0.1% across the frequency and thickness ranges of interest. Also, the results from Fig. 3(a) can be compared with those calculated using the classical skin-effect model (more traditionally associated with screening effectiveness calculations) using the following expression for the resulting error in shielding effectiveness E_{SE}:

$$E_{SE_{\mathrm{dB}}} = \left| \frac{SE_{dBo} - SE_{dBR}}{SE_{dBR}} \right| \cdot 100\% \tag{23}$$

(a)   (b)
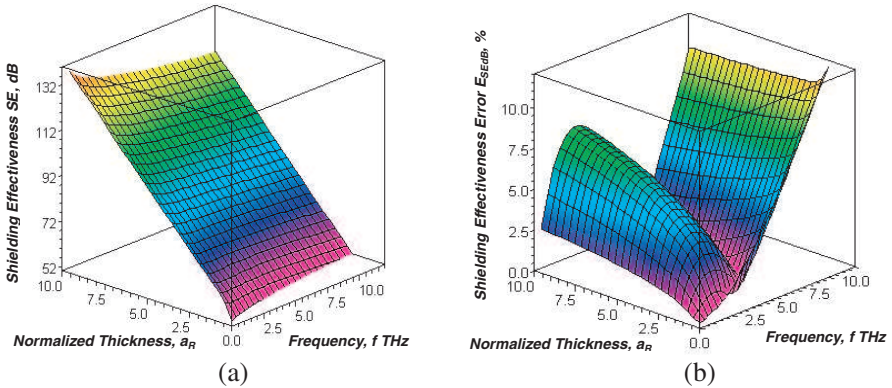
Figure 3. Screening effectiveness calculations: (a) using classical relaxation-effect model; (b) resulting error when compared to classical skin-effect model calculations.

where SE_{dBR} and SE_{dBo} are the screening effectiveness calculated using the classical relaxation-effect (11) and skin-effect (14) models, respectively. Using the engineering approach, it can be shown that the following more elegant expressions can be given for these figures of merit parameters, without introducing errors greater than 0.1%:

$$SE_{dBR} \cong 10 \log_{10} \left(\frac{8 \left(1 + Q_{cR}^2\right)/k_R^2}{\cosh(2a_R) - \cos(2a_R/Q_{cR})} \right)$$

$$\text{and } SE_{dBo} \cong 10 \log_{10} \left(\frac{16/k_o^2}{\cosh(2a_o) - \cos(2a_o)} \right) \tag{24}$$

The shielding effectiveness error results are represented by the contour plot shown in Fig. 3(b). A peak in the shielding effectiveness error occurs near $\omega\tau = 1/\sqrt{3}$; and increases in size with physical thickness to a value of 7.8% at $a_R = 10$. This peak is due to the associated error peak found in the absorption loss at exactly $\omega\tau = 1/\sqrt{3}$, since the classical relaxation-effect model predicts a smaller normal skin depth and, therefore, higher levels of absoprtion loss (when compared to the classical skin-effect model). It is interesting to note that $\omega\tau = 1/\sqrt{3}$ also corresponds to the turning point for wavelength against frequency within the metal, calculated using the classical relaxation-effect model [5]. Note that, beyond the region of this peak, the shielding effectiveness error increases almost linearly to a worst-case value of 11.7% at $T = l_m = 1.6\delta_{SR}(\omega\tau \cong 2.046)$.

2.2. Reflectance

Shields can also be exploited for their reflective properties, as found with quasi-optical components; their reflection characteristics can be represented by return loss. With reference to Fig. 1, return loss RL (i.e., the reflectance Γ) is the fraction of incident power P_i that is reflected back from the shield P_r and represented in decibels as:

$$RL_{\text{dB}} = -10 \log_{10} \left(\frac{P_r}{P_i} \right) = -10 \log_{10} (\Gamma) = -20 \log_{10} |S_{11}| \ \ [\text{dB}]$$

$$\text{where } RL = \Gamma_R = \begin{cases} |S_{11R}|^2 & \textit{for all } a_R \\ \cong |\rho_{1R}|^2 \approx \frac{k_R - 2}{k_R + 2} & \textit{for } a_R > 3 \end{cases} \tag{25}$$

Using (25) with (12), return loss has been calculated for gold at room temperature using the classical relaxation-effect model. The results are represented by the contour plot shown in Fig. 4(a). It can be seen that return loss RL_{dB} increases with frequency, as less electromagnetic energy is reflected back from the shield. Moreover, it decreases with

(a)   (b)
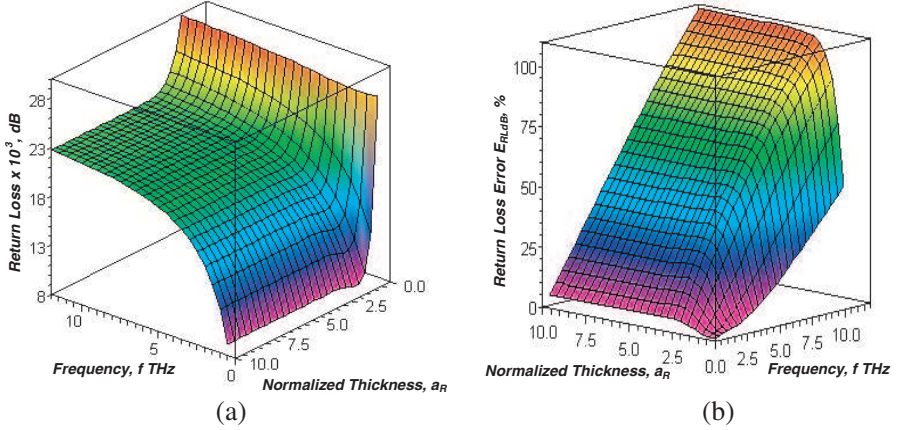
Figure 4. Return loss calculations: (a) using classical relaxation-effect model; (b) resulting error when compared to classical skin-effect model calculations.

increasing a_R, as the shield becomes more effective, until $a_R \approx 3$ where it is thickness invariant. Note that return loss calculations are sensitive to errors that result from making approximations and so no simplifying assumptions have been introduced.

The results from Fig. 4(a) can be compared with those calculated using the classical skin-effect model using the following expression for the resulting error in return loss E_{RL}:

$$E_{RL_{\mathrm{dB}}} = \left| \frac{RL_{dBo} - RL_{dBR}}{RL_{dBR}} \right| \cdot 100\% \tag{26}$$

where RL_{dBR} and RL_{dBo} are the return losses calculated using the classical relaxation-effect (12) and skin-effect (15) models, respectively. The return loss error results are represented by the contour plot shown in Fig. 4(b). It can be seen that the error increases almost linearly with frequency, to a worst-case value of 109% at $T = 10\delta_{SR}(\omega\tau \cong 2.046)$. This errors is relatively thickness invariant above $a_R \approx 3$, but falls dramatically below this value.

2.3. Absorptance

With reference to Fig. 1(a) and the law of conservation of energy, the power absorbed inside the metal shield P_a is given by the following:

$$P_a = P_i - P_t - P_r \tag{27}$$
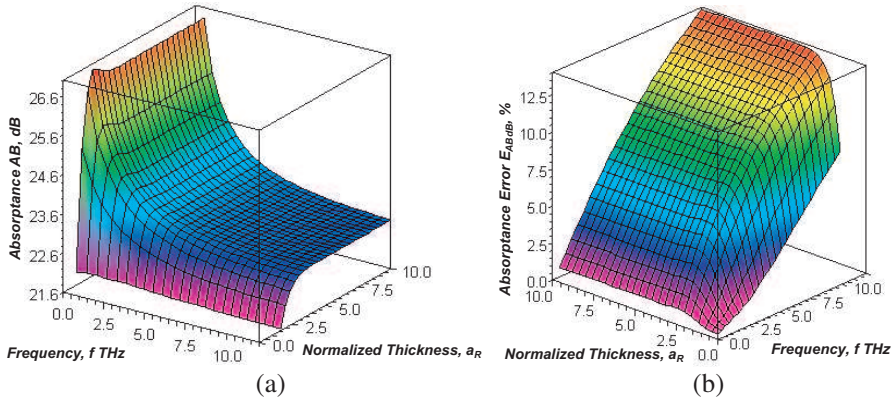
Figure 5. Absorptance calculations: (a) using classical relaxation-effect model; (b) resulting error when compared to classical skin-effect model calculations.

Absorptance AB is the fraction of incident power P_i that is absorbed within the shield P_a and is represented in decibels as:

$$AB_{\mathrm{dB}} = -10\log_{10}\left(\frac{P_a}{P_i}\right) = -10\log_{10}\left[1 - \left(\frac{P_t}{P_i}\right) - \left(\frac{P_r}{P_i}\right)\right]$$

$$= -10\log_{10}\left(1 - SE - RL\right) \tag{28}$$

$$AB = \begin{cases} 1 - |S_{21R}|^2 - |S_{11R}|^2 & \text{for all } a_R \\ \cong 1 - |\rho_{1R}|^2 \approx \frac{4}{k_R} \propto R_{SR} & \text{for } a_R > 3 \end{cases} \tag{29}$$

Using (28) with the exact expressions in (11) and (12), absorptance has been calculated for gold at room temperature using the classical relaxation-effect model. The results are represented by the contour plot shown in Fig. 5(a). It can be seen that absorptance AB_{dB} decreases with increasing frequency. Moreover, it increases with a_R, until $a_R \approx 3$, where it is thickness invariant. The results from Fig. 5(a) can be compared with those calculated using the classical skin-effect model using the following expression for the resulting error in return loss E_{AB}:

$$E_{AB\mathrm{dB}} = \left|\frac{AB_{dBo} - AB_{dBR}}{AB_{dBR}}\right| \cdot 100\% \tag{30}$$

where AB_{dBR} and AB_{dBo} are the absorptance calculated using the classical relaxation-effect (11) and (12) and skin-effect (14) and (15) models, respectively. The absorptance error results are represented by the contour plot shown in Fig. 5(b). It can be seen that this error contour is almost identical in shape to that for the return loss, shown

in Fig. 4(b). Here, the error increases almost linearly with frequency, to a worst-case value of 14% at $T = 10\delta_{SR}(\omega\tau \cong 2.046)$. This error is relatively thickness invariant above $a_R \approx 3$, but again falls dramatically below this value.

3. DETERMINING THE NORMAL SKIN DEPTH CROSS-OVER FREQUENCY

It has been shown that, when compared to that calculated using the classical relaxation-effect model, the classical skin-effect model predicts a larger normal skin depth below a certain cross-over frequency [5]. This means that if a metal shielding wall is designed using the classical skin-effect model, to a prescribed number of normal skin depths of physical thickness, then the measured power isolation will be higher than predicted using the classical relaxation-effect model; above the cross-over frequency, the converse is true. It was previously shown that [5]:

$$\delta_{SR} = \frac{1}{\Im\{\gamma_R\}Q_{cR}} = \Re\{\delta_{cR}\}\left(1 + \frac{1}{Q_{cR}^2}\right) \tag{31}$$

Therefore, the ratio of the two calculated normal skin depths can be represented by the following:

$$\chi = \frac{\alpha_o}{\alpha_R} = \frac{\delta_{SR}}{\delta_{So}} = \frac{\sqrt{Q_{cR}}}{2}\left(1 + \frac{1}{Q_{cR}^2}\right) \tag{32}$$

The cross-over frequency where $\chi \equiv 1$, $\omega\tau|_{\chi=1}$ can be found by replacing $Q_{cR} \Rightarrow (1 + \xi\,\omega\tau)^2$ [5], to give:

$$\therefore \omega\tau|_{\chi=1} = \frac{1 - \xi|_{\chi=1}}{\xi|_{\chi=1}^2} = 1.54369$$

$$\text{with} \qquad \xi|_{\chi=1} = (\omega\tau|_{\chi=1} - 1) = 0.54369 \tag{33}$$

For a fixed value of physical thickness, below $\omega\tau|_{\chi=1}$, the predicted absorption loss A_{dB} will be higher when calculated using the classical relaxation-effect model, compared to that from the classical skin-effect model; above $\omega\tau|_{\chi=1}$ the converse is true. However, the cross-over frequency will not be observed in the shielding effectiveness error contour plot given in Fig. 3(b). This is because the cross-over frequency in absorption loss is masked by the effects of cross-boundary reflections and, below $a_R \approx 3$, multiple reflections.

4. MODELLING OF METAL SHIELDING WALLS

It has previously been shown that, within the engineering approach, the predictive equivalent transmission line model can accurately solve

specific electromagnetic problems [5, 6]. This is the first time that a very practical application has been given, in the form of a metal shielding wall, using the model shown in Fig. 6.
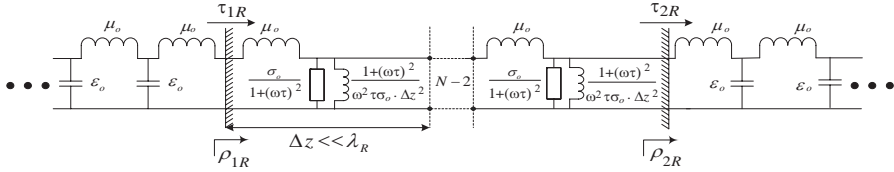
Figure 6. Equivalent transmission line model for predicting metal shielding behaviour, using the classical relaxation-effect model and showing expressions for the distributed-element parameters (e.g., $L_R \cdot \Delta z = 1.341$ [fH], $G_R \cdot \Delta z = 24.1$ [mS] and $L_{SHUNT\_R} \cdot \Delta z = 1.126$ [pH] at 5.865 THz for gold at room temperature [5, 6]).

Table 1. Comparison of modelled parameters for gold at room temperature, at 5.865 THz, determined from theory, direct $ABCD$ parameter matrix calculations and synthesized equivalent transmission line models using commercial circuit simulation software. The errors values are relative to those calculated using theory.

Parameters $a_R = 5,\ \omega\tau = 1,\ Z_T = \eta_o$	Theory	Synthesized Transmission Line ($N = 400$ *sections per wavelength*)			
		$ABCD$ **Parameter Matrix Calculations**		**Microwave Office®**	
		Value	Error [%]	Value	Error [%]
Z_{SR} [Ω]	0.4607904263 +j1.112446496	0.4607904255 +j1.112446495	-1.7×10^7 -0.9×10^7	---	---
$\gamma_R \cdot 5\delta_{SR}$ [$5\delta_{SR}^{-1}$]	5.0000 +j2.0711	5.0242 +j2.0807	+0.484 +0.464	---	---
$S_{21R} \cdot 10^5$	5.349 −j6.725	5.309 −j6.699	−0.748 −0.387	5.308 −j6.697	−0.766 −0.416
$\forall S_{21R}$ [°]	−51.499	−51.602	+0.200	−51.6	+0.196
Screening Effectiveness [dB]	81.317	81.363	+0.057	81.36	+0.053
S_{11R}	−0.9975 +j0.0059	−0.9975 +j0.0060	0.000 +1.695	−0.9975 +j0.0060	0.000 +1.695
Return Loss [dB]	0.02124	0.02124	0.000	0.02124	0.000

For example, at an arbitrary frequency of $\omega\tau = 1$, for gold at room temperature, the propagation constant is $\gamma_R(\omega\tau = 1) \cong 35.532 + j14.718$ [μm^{-1}] and, therefore, the normal skin depth $\delta_{SR}(\omega\tau = 1) \cong 28.1429$ [nm]. Also, when one wavelength $\lambda_R(\omega\tau = 1) = 2\pi\delta_{SR}(\omega\tau = 1)Q_{cR}(\omega\tau = 1) \cong 426.8983$ [nm] is divided up into $N = 400$ sections

then $\Delta z(\omega\tau = 1) \cong 1.067245$ [nm]. Thus, for $a_R = 5$, $5\delta_{SR}(\omega\tau = 1)/\Delta z(\omega\tau = 1) \cong 132$ sections are needed to synthesize the equivalent transmission line model for the metal shielding wall. Theoretical values for power isolation and reflectance are 81.32 dB and 99.504%, respectively. These values can be compared with those extracted from the $ABCD$ parameter matrix calculations of 81.36 dB and 99.504%, respectively. Therefore, from these results and those shown in Table 1, the validity of employing the equivalent transmission line model to predict both the transmittance and reflectance characteristics of a room temperature THz metal shield is proven.

5. CONCLUSIONS

This paper has applied the recently introduced electrical engineering approach to investigate room temperature THz metal shielding, using the accurate classical relaxation-effect frequency dispersion model. It has been found that, with the simplest case of a uniform plane wave at normal incidence to an infinite single planar shield in air, all figure of merit parameters for the shield can be accurately characterized. The errors introduced by adopting the traditional and much simpler classical skin-effect model have also been quantified. It was found that the errors for screening effectiveness and absorptance are much less than those found with metal-pipe rectangular waveguides and associated cavity resonators; while those for return loss are comparable and can exceed 100% within the THz frequency and practical thickness ranges of interest [4, 6]. In addition, errors resulting from adopting well-established approximations have also been investigated and quantified.

Furthermore, an equivalent transmission line model was synthesized and simulated. The results were compared with theory and through the use of commercial circuit simulation software. It was found that this modelling approach accurately predicts the behaviour of the THz metal shielding structure.

In summary, it has been seen that the engineering approach allows analytical expressions to be greatly simplified and predictive models to be synthesized, allowing a much deeper insight to be made into the behaviour of room temperature THz metal shielding. For example, it is shown that figures of merit and associated errors (resulting from the use of different classical frequency dispersion models) become essentially thickness invariant when the physical thickness of the shield is greater than 3 normal skin depths. Therefore, the only figure of merit to benefit from a thicker shield is the screening effectiveness.

ACKNOWLEDGMENT

REFERENCES

1. Lucyszyn, S., "Investigation of anomalous room temperature conduction losses in normal metals at terahertz frequencies," *IEE Proc. — Microwaves, Antennas and Propagation*, Vol. 151, No. 4, 321–329, 2004.

2. Lucyszyn, S., "Investigation of Wang's model for room temperature conduction losses in normal metals at terahertz frequencies," *IEEE Trans. on Microwave Theory Tech.*, Vol. 53, 1398–1403, 2005.

3. Lucyszyn, S., "Evaluating surface impedance models for terahertz frequencies at room temperature," *PIERS Online*, Vol. 3, No. 4, 554–559, 2007.

4. Zhou, Y. and S. Lucyszyn, "HFSS$^{\text{TM}}$ modelling anomalies with THz metal-pipe rectangular waveguide structures at room temperature," *PIERS Online*, Vol. 5, No. 3, 201–211, 2009.

5. Lucyszyn, S. and Y. Zhou, "Engineering approach to modelling frequency dispersion within normal metals at room temperature for THz applications," *Progress In Electromagnetics Research*, PIER 101, 257–275, 2010.

6. Lucyszyn, S. and Y. Zhou, "THz applications for the engineering approach to modelling frequency dispersion with normal metals at room temperature," *PIERS Online*, Vol. 6, No. 3, 293–299, 2010.

7. Paul, C. R., *Introduction to Electromagnetic Compatibility*, John Wiley & Sons, New York, 1992.

8. "Shielding theory," http://www.cvel.clemson.edu/emc/tutorials/ Shielding01/Shielding_Theory.html.

9. IEEE Std 299-1997, "IEEE Standard method for measuring the effectiveness of electromagnetic shielding enclosures," Dec. 1997.